Journal of Earth and Planetary System Science
Volume 1, Issue 1, 1-18.
E-ISSN: 2963-1963
https://journal.gomit.id/jepss/index

Tropical Cyclone Senyar: Cyclone Structure and Topographic Remote Rainfall Extremes in North Sumatera

Muhammad Ansori Hasibuan*
Climatology Station of North Sumatera Utara,
INDONESIA

*** Corresponding author:**
Muhammad Ansori Hasibuan, Climatology Station of North Sumatera Utara, INDONESIA. ✉ ansori.hasibuan@bmkg.go.id

Article Info

Article history:

Received: Juni 18, 2026
Revised: Juli 03, 2026
Accepted: Juli 14, 2026
(Cambria 9)

Keywords:

Cyclone
North Sumatera
Rainfall
Senyar
Topographic

Abstract

Background: Tropical cyclones forming within or near the Malacca Strait can trigger extreme rainfall over North Sumatra through interactions between cyclone dynamics, atmospheric moisture transport, and the orographic effects of the Bukit Barisan mountain range. However, the mechanisms linking Tropical Cyclone Senyar to remote orographic extreme rainfall remain poorly understood.
Aims: This study investigates the relationship between the structure of Tropical Cyclone Senyar and remote orographic extreme rainfall over North Sumatra.
Methods: ECMWF reanalysis data were processed using Python-based computational and visualization tools. The analyzed variables included total precipitation, 10-m zonal and meridional wind components, mean sea level pressure, specific humidity, and vertical velocity at 37 pressure levels. Topographic influences were represented using the 30-m SRTM Digital Elevation Model
Result: During 21–30 November 2025, Tropical Cyclone Senyar produced total rainfall accumulations of 117.16–871.48 mm (mean: 340.25 mm) and a maximum daily rainfall of 327.01 mm day^{-1}, with a minimum mean sea level pressure of 1009.64 hPa. Extreme rainfall (>150 mm day^{-1}) occurred mainly over Sibolga, North Tapanuli, Langkat, Medan, and Deli Serdang. Strong moisture transport, organized moisture flux corridors, localized moisture convergence, and persistent negative omega values at 500 hPa promoted deep convection. Rainfall maxima coincided with the orographic forcing zone along the Bukit Barisan range.
Conclusion: The integrated analysis demonstrates that Tropical Cyclone Senyar, moisture transport, vertical atmospheric dynamics, and orographic forcing acted synergistically to generate remote extreme rainfall over North Sumatra, providing new insights into extreme precipitation mechanisms in the equatorial maritime region.

To cite this article: Hasibuan, A.M. (2026). Tropical Cyclone Senyar: Cyclone Structure and Topographic Remote Rainfall Extremes in North Sumatera. *Journal of Earth and Planetary System Science,* 1(1),1-18

INTRODUCTION

Tropical cyclones generally develop over warm oceanic regions with sufficiently large planetary vorticity; therefore, their occurrence near the equator, particularly over the Malacca Strait, is relatively rare (Gray, 1975), (Wang & Wu, 2004), (Surinati & Kusuma, 2018), (Suhardi et al., 2020). However, in late November 2025, Tropical Cyclone Senyar developed from the tropical disturbance 95B over the eastern waters of Aceh and evolved into one of the most unusual meteorological events in the maritime Southeast Asian region (Lui et al., 2026), (Abdillah et al., 2026). The cyclone formed, propagated, and interacted within a region that is not climatologically recognized as a primary tropical cyclone track corridor (Syahreza et al., 2026), (Sobel et al., 2021). The Indonesian Agency for Meteorology, Climatology, and Geophysics (BMKG) reported that the system was officially classified as Tropical Cyclone Senyar on 26 November 2025, with a central pressure of approximately 998 hPa and maximum sustained winds of about 43 knots, and was associated with a marked increase in very heavy to extreme rainfall over Aceh and North Sumatra (Syahreza et al., 2026).

The uniqueness of Senyar lies not only in its anomalous genesis but also in the spatial distribution of extreme rainfall, which does not strictly follow proximity to the cyclone center. In many cases, the highest rainfall intensities do not occur near the circulation core but instead develop at considerable distances from the system center due to the combined effects of spiral rainbands, moisture advection, mesoscale convergence, and orographic lifting (Schumacher & Rasmussen, 2020). This phenomenon is particularly relevant in North Sumatra, a region characterized by complex topography associated with the Bukit Barisan mountain range, which extends parallel to the western coast of Sumatra and creates a steep elevation gradient from coastal areas to the interior (Sheil, 2026). Under highly moist atmospheric conditions and persistent onshore flow, this terrain can enhance rainfall through mechanisms of forced ascent and topographic locking, resulting in extreme precipitation accumulation even when the cyclone center is relatively distant (Chen, 2025).

The impacts of Senyar over North Sumatra indicate that the relationship between tropical cyclones and extreme rainfall in maritime tropical regions cannot be explained solely by storm intensity parameters such as minimum pressure or maximum wind speed. BMKG reported extreme rainfall during 25-27 November 2025 at several locations, including Langkat (376.8 $mm.day^{-1}$) and Central Tapanuli (133 $mm.day^{-1}$), demonstrating that the system was capable of producing extreme precipitation in areas geographically situated outside the classical eyewall zone and more strongly influenced by regional moisture flow configuration and interactions with local topography (Rahman et al., 2024).

In general, rainfall associated with tropical cyclones is governed by a combination of synoptic-, mesoscale-, and local-scale processes. At the synoptic scale, precipitation distribution is influenced by the cyclone circulation structure, wind field asymmetry, system translation, vertical wind shear, and the availability of ocean–atmosphere energy (Klotzbach et al., 2022), (Wadler et al., 2023). Recent studies indicate that Tropical Cyclone Senyar was a highly unusual system, as it represents one of the first observed tropical cyclones to develop within the Malacca Strait and subsequently propagate in an atypical eastward or westward direction in a region very close to the equator, suggesting a distinctive regional atmospheric configuration during the event (Lui et al., 2026).

In tropical cyclone literature, storm structure is commonly analyzed through components such as the circulation center, spiral rainbands, convective bursts, warm-core signatures, vorticity maxima, moisture flux convergence, and the distribution of convective clouds observed from infrared and microwave satellite imagery, as well as reanalysis products, (Kidder et al., 2000), (Yang, 2026), (Chen et al., 2026). These structural features govern the location and efficiency of rainfall production, but are not necessarily collocated with the areas of maximum precipitation over land (Chakraborty et al., 2026). In many coastal and mountainous regions, maximum rainfall is primarily controlled by the interaction between moisture-laden cyclonic flow and local topography, rather than solely by the intensity of the storm core (Katru et al., 2025), (Kim et al., 2025).

The role of topography in rainfall enhancement has long been recognized in tropical meteorology. When moisture-laden airflow from the ocean is forced to ascend along mountainous slopes, adiabatic cooling and condensation are intensified, often resulting in substantially higher rainfall compared to adjacent lowland areas (French et al., 2018), (Junquas et al., 2018), (Sandu et al., 2019). In northern Sumatra, the Bukit Barisan mountain range serves as a major orographic barrier to westerly and northwesterly flows originating from the Indian Ocean and the Malacca Strait (Ramadhan et al., 2026). Under strong synoptic disturbances such as tropical cyclones, the influence of orography can be significantly amplified due to more persistent and organized low-level moisture supply and convergence (Shu et al., 2018), (Lentink et al., 2018).

Studies on cyclone-induced remote rainfall further indicate that extreme precipitation can occur at distances of several hundred kilometers from the storm center (Arakane et al., 2019), (Mazza & Chen, 2023). This concept is particularly relevant for regions that are not directly traversed by the cyclone track but remain within zones of moisture advection, outer rainbands, or flow curvature (Vo & Liou, 2024), (Zhi-ying et al., 2017). In the context of South Asia and the northern Indian Ocean, previous studies have shown that tropical cyclones can trigger extreme rainfall over inland areas far from the storm core through mechanisms such as moisture conveyor belts, interactions with the monsoon trough, and enhancement of localized convergence (Chen et al., 2021), (Khouakhi et al., 2017). This is consistent with broader findings in the North Indian Ocean basin, where, despite lower cyclone frequency compared to other basins, these systems often produce highly complex and impactful rainfall patterns (Singh et al., 2000), (Deshpande et al., 2021), (Balaji et al., 2018), (Hoarau et al., 2012).

However, much of the existing literature remains focused on cyclone track and intensity, coastal or maritime impacts, or large-scale rainfall totals (Leroux et al., 2018) , (Needham et al., 2015). Studies explicitly linking internal cyclone structure with remote orographic rainfall extremes at provincial or watershed scales remain relatively limited, particularly in western Indonesia, which is climatologically situated within the equatorial zone. In the case of Senyar, the occurrence of repeated extreme rainfall over North Sumatra for several consecutive days, even when the cyclone center was not directly overhead, underscores the need for an integrated approach that combines cyclone structure, moisture transport, spatial rainfall patterns, and topographic controls within a unified analytical framework.

This study aims to examine the relationship between the structure of Tropical Cyclone Senyar and remote orographic extreme rainfall over North Sumatra, with particular emphasis on how the dynamical characteristics of the storm interact with regional topography to produce non-uniform rainfall distributions. Within this context, Tropical Cyclone Senyar is treated not merely as a rare extreme weather event, but as a natural experiment for understanding how tropical cyclones developing in near-equatorial environments can generate highly localized, topographically modulated extreme rainfall. By integrating cyclone structure analysis with rainfall response over North Sumatra, this study seeks to contribute to the broader literature on tropical cyclone rainfall, orographic hydrometeorology, and impact-based forecasting in the Indonesian maritime region.

METHOD

This study employed a quantitative descriptive approach with a case study design to investigate the atmospheric conditions associated with the weather event during the study period (Day et al., 2013). The research site is located in North Sumatra Province, with data collection coordinates ranging from 6° N to 0.5° N and 94° E to 101° E. The analysis was based on secondary data derived from ECMWF reanalysis datasets, with emphasis on the spatial and temporal variability of selected meteorological parameters relevant to the event. The primary research instrument consisted of ECMWF reanalysis data, which were processed and analyzed using Python-based computational and visualization tools. The meteorological variables used in this study are presented in **Table 1**, and the analysis covered the period from 21-30 November 2026.

Furthermore, this study utilizes DEM data for the North Sumatra region to examine elevation and topographic characteristics across different areas, particularly along the Bukit Barisan mountain range that traverses North Sumatra accessed via a link https://www.indonesia-geospasial.com/2020/01/download-dem-srtm-30-meter-se-indonesia.html. The research procedures included several stages data collection, selection of relevant atmospheric variables, data processing, visualization, and interpretation of atmospheric conditions. These steps were carried out systematically to examine the evolution and interaction of atmospheric parameters before, during, and after the event.

Table 1. Research Variable

Variable	Unit	Temporal resolution	Horizontal resolution	Vertical resolution
Total precipitation (tp)	mm	hourly	0.25° x 0.25°	-
10m u-component of wind (u10)	$m.s^{-1}$	hourly	0.25° x 0.25°	-
10m v-component of wind (v10)	$m.s^{-1}$	hourly	0.25° x 0.25°	-
Mean sea level pressure (msl)	Pa	hourly	0.25° x 0.25°	-
Specific Humidity (q)	$kg.kg^{-1}$	hourly	-	37 pressure levels
Vertical Velocity (w)	$Pa.s^{-1}$	hourly	-	37 pressure levels

The data analysis was conducted using descriptive, temporal, and spatial approaches. Temporal analysis was applied to identify changes in atmospheric conditions over time, while spatial analysis was used to examine the distribution and extent of meteorological features across the study domain. These analytical approaches were intended to provide a comprehensive understanding of the atmospheric processes associated with the event.

This study was limited to the use of ECMWF reanalysis data and the selected meteorological parameters within the period 21-30 November 2026. Therefore, the findings represent atmospheric conditions only within the specified temporal and spatial domain. A methodological limitation of this study is that reanalysis data are not direct observations, but rather model-assimilated products, which may not fully resolve small-scale or localized atmospheric processes. In addition, the absence of detailed integration with other supporting datasets, such as weather radar, satellite imagery, and in-situ observations, may reduce the overall comprehensiveness of the atmospheric interpretation.

Cyclone Structure Analysis

The synoptic structure of Tropical Cyclone Senyar was characterized using mean sea level pressure (MSLP) and 10-m wind fields from the reanalysis dataset (Cornes et al., 2012). MSLP was converted from Pa to hPa as:

$$MSLP_{(hPa)} = \frac{MSLP_{(Pa)}}{100} \quad \text{.......(1)}$$

where $MSLP_{(hPa)}$and $MSLP_{(Pa)}$ denote pressure in hectopascal and Pascal, respectively. Wind speed was computed from the zonal (u) and meridional (v) wind components:

$$V = \sqrt{u^2 + v^2} \quad \text{.......(2)}$$

where $V$is wind speed (m.s^{-1}), and u and v are the horizontal wind components (m.s^{-1}) [45]. The cyclone center was defined as the location of minimum pressure within the study domain:

$$P_c = \min[MSLP(x,y)], (x_c, y_c) = \arg\min[MSLP(x,y)] \quad \text{.......(3)}$$

where P_c is the central pressure and (x_c, y_c) represents the cyclone center coordinates. The MSLP field was visualized using isobars, and the wind field was displayed as vectors.

Rainfall Analysis

To investigate the precipitation response associated with Tropical Cyclone Senyar, daily rainfall data were analyzed over the study domain for the period 21–30 November 2025. Two rainfall indicators were derived to characterize the event: total accumulated rainfall and maximum daily rainfall (Zhou et al., 2008). The total accumulated rainfall at each grid point was calculated as:

$$R_{\text{total}}(x,y) = \sum_{t=1}^{n} R(x,y,t) \quad \text{.......(4)}$$

where $R(x,y,t)$ represents daily rainfall (mm) at grid point (x, y) on day t, and n is the number of days included in the event period.

To identify the spatial pattern of short-duration rainfall extremes, the maximum daily rainfall was computed as:

$$R_{\max}(x,y) = \max_{t=1,\dots,n}[R(x,y,t)] \quad \text{.......(5)}$$

where $R_{\max}(x,y)$ denotes the highest daily rainfall value recorded at each grid point during the event period.

Moisture Transport Analysis

To investigate the atmospheric moisture pathways associated with Tropical Cyclone Senyar, horizontal moisture transport was analyzed using specific humidity and near-surface wind components extracted from the reanalysis dataset. The selected variables were averaged over the cyclone influence period to represent the mean moisture transport pattern during the event (Glaskova et al., 2007).

The zonal and meridional components of moisture flux were calculated as:

$$Q_u = q \cdot u \quad \text{......(6)}$$

$$Q_v = q \cdot v \quad \text{......(7)}$$

where q denotes specific humidity (kg.kg^{-1}), and u and v represent the zonal and meridional wind components (m.s^{-1}), respectively. The magnitude of the horizontal moisture flux was then computed as:

$$\mid Q \mid = \sqrt{Q_u^2 + Q_v^2} \quad \text{......(8)}$$

This parameter was used to identify the spatial intensity of moisture transport associated with the cyclone circulation. To further examine regions favorable for moisture accumulation and enhanced precipitation, moisture convergence was estimated as the negative horizontal divergence of the moisture flux field:

$$MC = -\left(\frac{\partial Q_u}{\partial x} + \frac{\partial Q_v}{\partial y}\right) \quad \text{......(9)}$$

Positive values of MC indicate convergent moisture transport, which is commonly associated with upward motion and convective development, whereas negative values indicate moisture divergence.

Vertical Motion Analysis

The vertical structure of atmospheric motion associated with Tropical Cyclone Senyar was analyzed using vertical velocity (omega, ω) at the 500 hPa pressure level (Smith, 1971). Vertical velocity in pressure coordinates is defined as:

$$\omega = \frac{Dp}{Dt} \quad \text{......(10)}$$

where ω represents the rate of change of pressure with time (Pa.s^{-1}). Negative values of ω indicate upward motion, while positive values indicate subsidence.

To characterize the mean vertical motion during the cyclone influence period, the vertical velocity field was averaged over time:

$$\bar{\omega}(x, y) = \frac{1}{n}\sum_{t=1}^{n} \omega(x, y, t) \quad \text{......(11)}$$

where n denotes the number of time steps in the analysis period.

The 500 hPa level was selected to represent mid-tropospheric dynamics, which are closely related to large-scale ascent and deep convection. In cases where the exact 500 hPa level was not available, the nearest pressure level was selected based on:

$$p^* = \arg\min \mid p - 500 \mid \quad \text{......(12)}$$

The resulting vertical velocity field was analyzed spatially to identify regions of persistent ascent associated with enhanced convection and rainfall during the influence of Tropical Cyclone Senyar.

Topographic and Orografi Influence on Rainfall

To assess the role of terrain in modulating rainfall during the influence of Tropical Cyclone Senyar, the spatial distribution of rainfall was compared with regional topography over North Sumatra (Wilks, 2011). Mean daily rainfall was calculated as:

$$\bar{R}(x, y) = \frac{1}{n}\sum_{t=1}^{n} R(x, y, t) \quad \text{......(13)}$$

where $\bar{R}(x, y)$denotes mean daily rainfall (mm.day^{-1}) at grid point (x‚y), $R(x, y, t)$is the daily rainfall, and $n$is the number of days in the analysis period.

Topographic information was obtained from a Digital Elevation Model (DEM). To match the spatial scale of the meteorological analysis and reduce computational complexity, the elevation field was resampled using spatial averaging (Purkis & Klemas, 2011):

$$Z_r(x, y) = \mathcal{R}[Z(x, y)] \quad \text{...(14)}$$

where $Z(x, y)$is the original elevation and $Z_r(x, y)$is the resampled terrain field.

For visualization purposes, the resampled elevation was further smoothed using a Gaussian filter:

$$Z_s(x, y) = G_\sigma * Z_r(x, y) \quad \text{...(15)}$$

where $G_\sigma$represents the Gaussian smoothing kernel (Bracewell & Bracewell, 1986). The smoothed topographic field was then overlaid with the rainfall distribution to examine the spatial correspondence between rainfall maxima and elevated terrain, particularly along the Bukit Barisan mountain range.

RESULTS AND DISCUSSION

Results

Cyclone Structure Analysis

Mean sea level pressure (MSLP) during Tropical Cyclone Senyar reached 1011.2 hPa, with values ranging from 1009.6 to 1016 hPa (**Fig. 1**). The minimum MSLP was recorded at 1009.64 hPa, located at 2.50°S, 101.00°E. The mean surface wind speed was 4.04 m.s^{-1} (range: 0.01–8.89 m s^{-1}), with a maximum of 8.89 m.s^{-1} observed at 6.00°S, 98.50°E. The prevailing wind flow was predominantly westerly, directing toward the western coastal regions of North Sumatra, particularly over Sibolga and North Tapanuli.

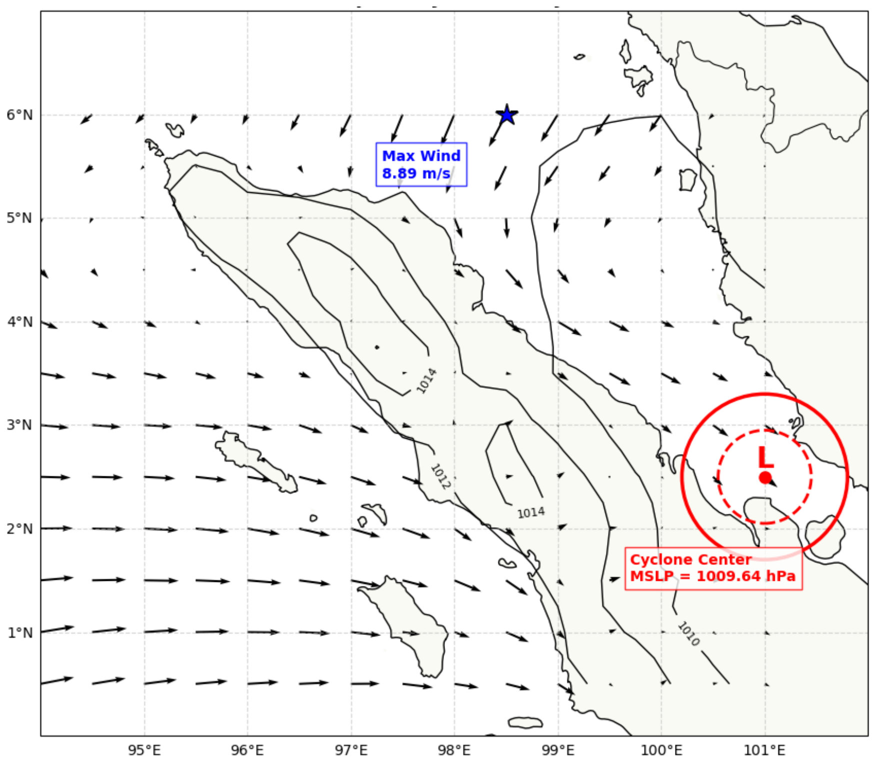

Figure 1. Mean sea level pressure and Surface wind Tropical Cyclone Senyar (period from 21-30 November 2026)

Based on the flow direction, the wind field was influenced by the trailing circulation of Tropical Cyclone Senyar, propagating toward the western coastal sector. The presence of the Bukit Barisan mountain range acted as a topographic barrier, modifying the airflow and redirecting it along the western coast of Sumatra. This orographic interaction likely contributed to enhanced rainfall intensity, which was associated with flood and landslide occurrences in several areas along the western coast of North Sumatra, including Sibolga, North Tapanuli, and Mandailing Natal. A similar mechanism was observed over the eastern sector, where the circulation associated with Cyclone Senyar advected moisture through the Malacca Strait toward the Malaysian Peninsula, corresponding to a low-pressure system. This propagation was associated with increased rainfall over eastern regions such as Langkat, Deli Serdang, and Medan, where flooding events were reported during the same period.

Rainfall Analysis

Total accumulated rainfall associated with Tropical Cyclone Senyar ranged from 117.16 to 871.48 mm, with a mean of 340.25 ± 168.59 mm (**Fig. 2**). The red contour delineates areas receiving ≥300 mm during the period 21–30 November 2026. Elevated rainfall totals were observed across most parts of North Sumatra, with pronounced maxima along both the western and eastern coastal regions. Maximum daily rainfall varied between 31.02 and 327.01 mm (moderate to extreme category), with a mean of 100.72 ± 55.25 mm (**Fig. 3**). Extreme daily rainfall (>150 mm.day^{-1}) was identified over Sibolga, North Tapanuli, Langkat, Medan, and Deli Serdang. The peak values for both accumulated and daily rainfall were co-located at 4.50°N, 99.00°E.

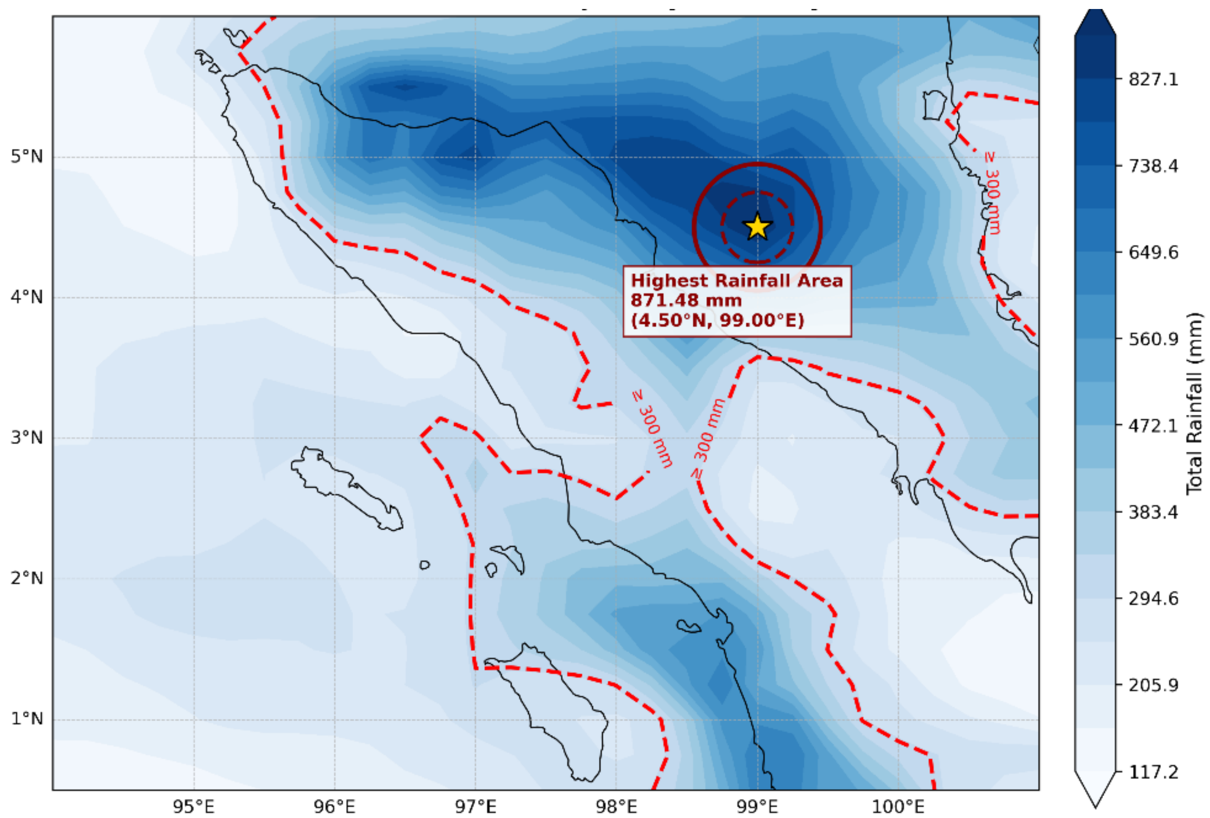

Figure 2. Total Rainfall Distribution and High Rainfall Area 21 – 30 November 2025

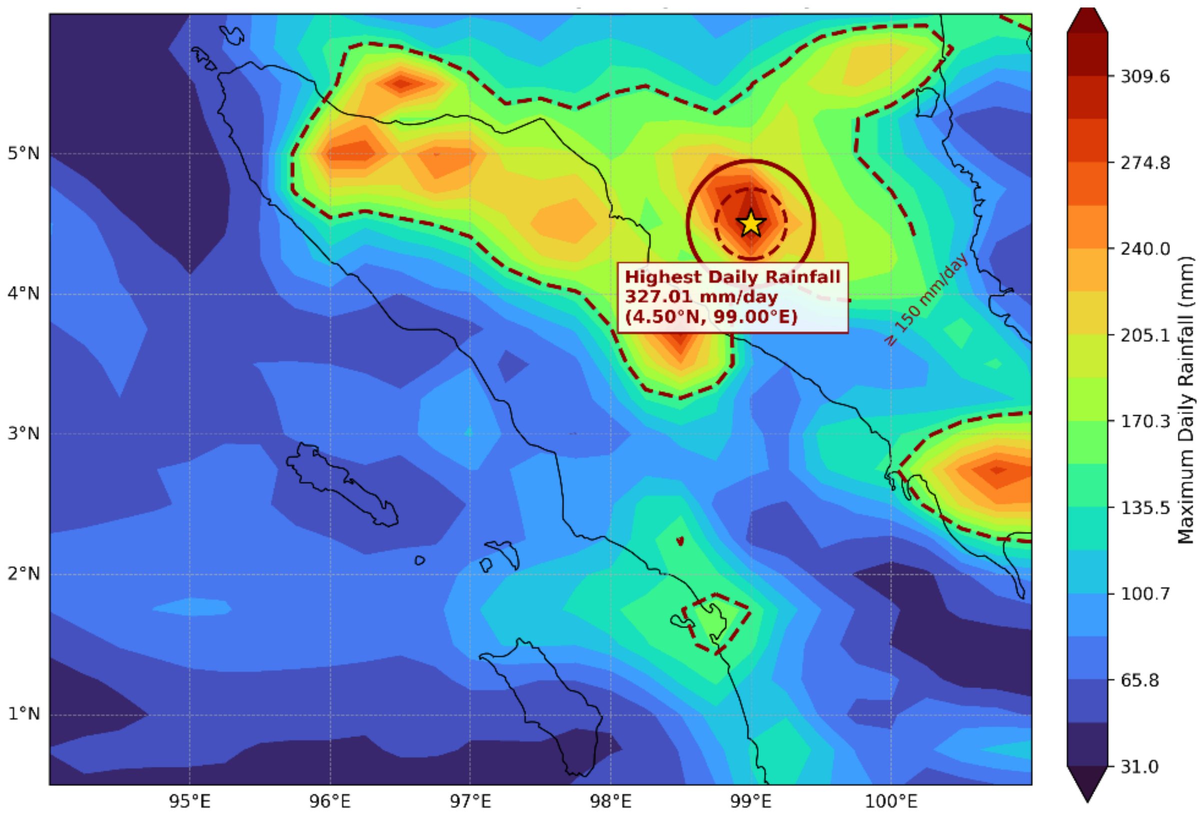

Figure 3. Maximum Daily Rainfall Distribution 21 – 30 November 2025

Moisture Transport Analysis

The distribution of integrated vapor transport (IVT) indicates a structured pathway of moisture advection toward the study domain during the influence of Tropical Cyclone Senyar (**Fig. 4a**). The domain-averaged IVT magnitude reached 4.64×10^{-2}, with a maximum value of 8.49×10^{-2}located at (0.75°N, 97.25°E), reflecting a localized intensification of horizontal moisture flux over the adjacent oceanic sector. The relatively high standard deviation (2.66×10^{-2}) suggests substantial spatial variability, with approximately 23.2% of the domain exceeding the threshold of mean plus one standard deviation, indicating confined regions of enhanced moisture transport rather than uniform distribution.

The spatial structure of moisture flux is characterized by coherent and concentrated flow patterns, as reflected by the alignment of transport pathways toward the northern–western and central parts of the domain (**Fig. 4b**). This configuration implies that moisture advection is organized along preferential corridors, supporting sustained horizontal transport from oceanic source regions into the study area. Moisture convergence exhibits a domain-mean value of -1.35×10^{-7}, indicating near-neutral conditions at the large scale, while localized maxima reach 3.82×10^{-6}at (2.75°N, 97.75°E), highlighting distinct zones of moisture accumulation (**Fig. 4c**). The associated standard deviation (1.27×10^{-6}) further reflects spatial heterogeneity, with only 11.8% of the domain exceeding the defined threshold, suggesting that convergence is confined to limited areas. These localized convergence features are consistent with regions where horizontal moisture flux is effectively concentrated, indicating spatially selective accumulation of atmospheric moisture.

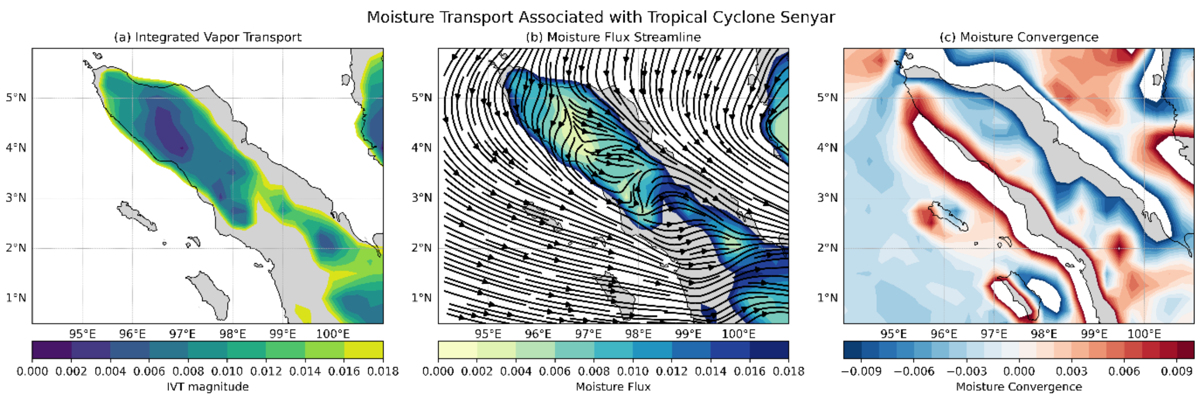

Figure 4. (a) Integrated Vapor Transport; (b) Moisture lux Streamline; (c) Moisture Convergence

Vertical Motion Analysis

The distribution of vertical velocity at the 500 hPa level during the Tropical Cyclone Senyar event indicates a predominance of ascending motion across most of North Sumatra, as evidenced by negative omega values (ω < 0 Pa.s^{-1}) (**Fig. 5**). In atmospheric dynamics, this condition reflects active upward transport of air masses within the mid-troposphere, representing a key indicator of enhanced convection and cloud development at the synoptic scale. Spatially, the strongest ascending core is identified over the western to northwestern sectors of North Sumatra, particularly over the adjacent offshore region west of Sibolga, and extends inland toward the northern–central parts of the domain. The minimum vertical velocity reaches approximately ω < −0.45 Pa.s^{-1}, indicating intense and relatively organized updrafts. This zone encompasses areas associated with northern Tapanuli and extends toward parts of Langkat, Deli Serdang, and Medan. The relatively large magnitude of omega at 500 hPa suggests that vertical motion is not confined to the lower troposphere but has developed into the mid-levels, thereby supporting the formation of deep convective systems.

This pattern is significant, as the 500 hPa level serves as a representative layer for assessing the persistence of vertical convection. The widespread and continuous occurrence of negative omega values at this level indicates the presence of mature convective processes rather than shallow convection, with the potential to produce substantial precipitation. In this context, the atmospheric column over North Sumatra during the cyclone period can be characterized as dynamically active and vertically unstable, favoring the development of moderate to heavy rainfall. Furthermore, the spatial concentration of stronger negative omega values over the western and northern sectors suggests a non-uniform atmospheric response to the cyclone. This distribution implies a more effective focus of convergence and upward motion in these regions, likely influenced by the interaction between large-scale cyclonic circulation, moisture supply from the Indian Ocean, and orographic forcing associated with the Bukit Barisan mountain range. Such conditions enhance the likelihood of adiabatic cooling, condensation, and the growth of deep convective clouds in these areas.

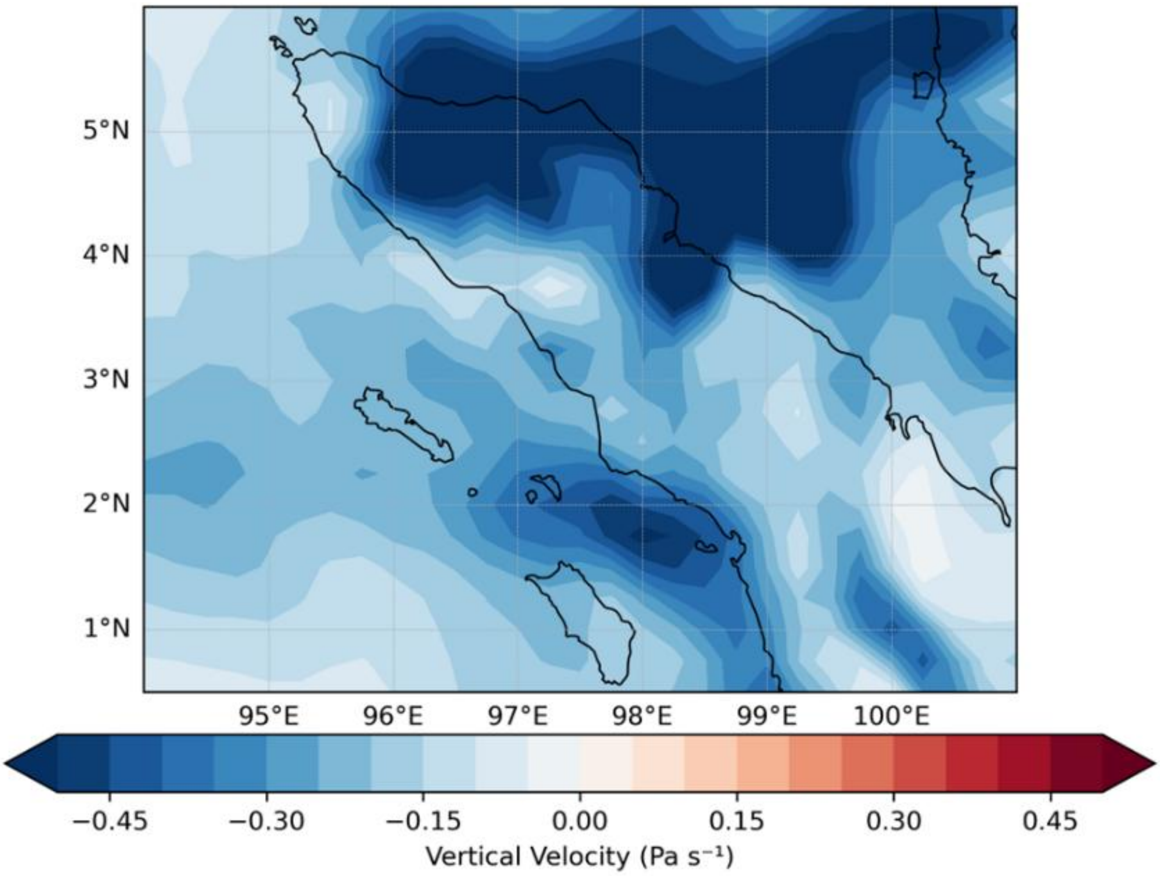

Figure 5. Vertical Velocity 500 hPa

In contrast, the eastern and southeastern parts of the domain exhibit weaker and near-neutral vertical velocity values, indicating that vertical lifting mechanisms in these regions are less pronounced compared to the western–northern sector. This spatial contrast suggests that the influence of Tropical Cyclone Senyar on rainfall generation over North Sumatra was localized rather than uniformly distributed across the domain. Consequently, precipitation during this period was likely concentrated in areas corresponding to the strongest negative omega anomalies. The 500 hPa vertical velocity pattern further indicates that rainfall occurrence was not solely driven by elevated moisture availability but also strongly supported by persistent vertical dynamical forcing. Therefore, this parameter provides clear evidence that the dominant rainfall-generating mechanism during the event was governed by large-scale to mesoscale atmospheric ascent, facilitating the development of deep convection.

Topographic Influence on Rainfall

The spatial distribution of daily rainfall indicates that precipitation during the Tropical Cyclone Senyar event was not uniformly distributed across North Sumatra. The highest rainfall intensities were identified over the northern to northeastern sectors, with values ranging from approximately 66.58-80.29 mm.day^{-1}. This zone encompasses the northeastern coastal region and adjacent northern inland areas, representing the core of maximum precipitation. In addition, relatively high rainfall extends along a northwest–southeast oriented band, particularly across the central to eastern parts of the domain. This configuration forms a distinct rainfall corridor, indicating localized enhancement of precipitation associated with regional-scale influences. In contrast, the southwestern sector and parts of the offshore western region exhibit lower rainfall amounts, generally within the range of 11.72-39.15 mm.day^{-1}. The spatial pattern reveals a clear rainfall gradient between mountainous regions and surrounding areas. Higher rainfall accumulation is observed in proximity to complex topography, particularly along slopes and ridges associated with the Bukit Barisan mountain range. Conversely, several lowland areas and open ocean regions display comparatively lower intensities relative to terrain-influenced regions (**Fig. 6**).

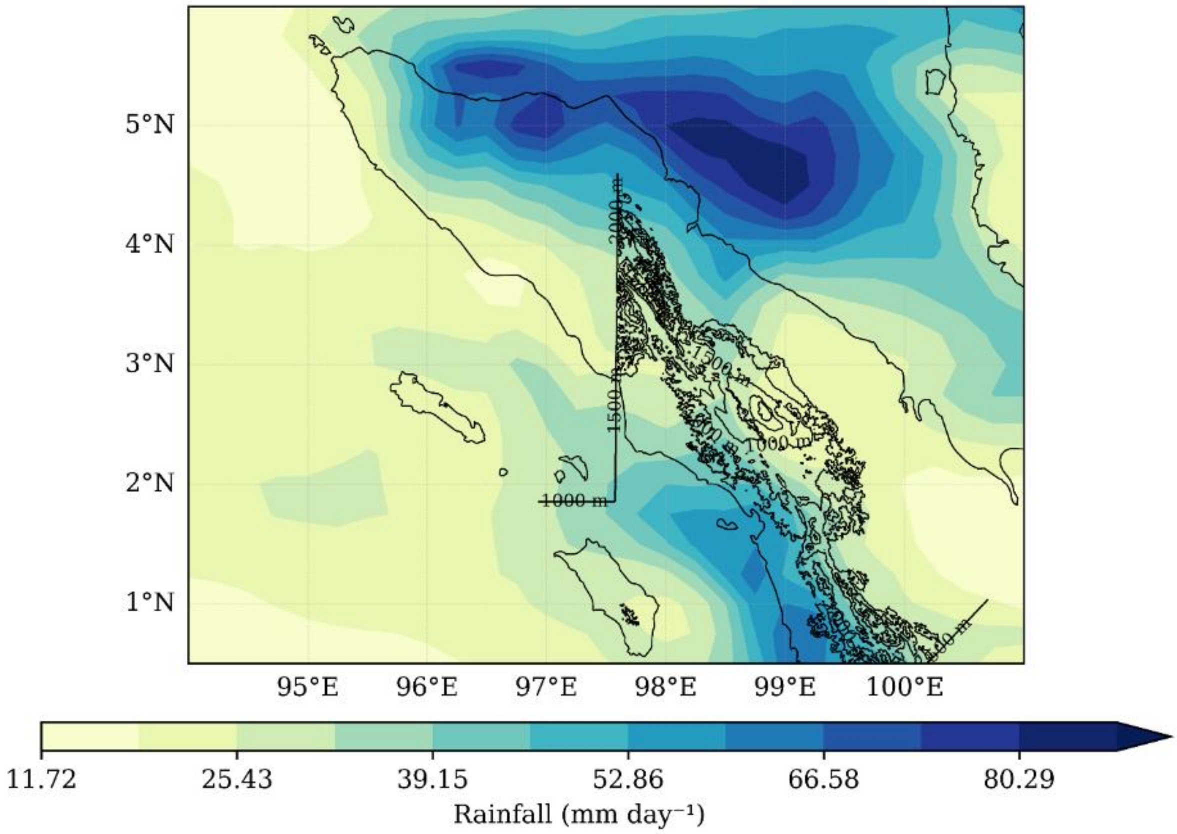

Figure 6. Spatial Distribution of Rainfall and Orographic Influence North Sumatra

Orographic Influence on Rainfall Distribution

The cross-sectional profile of rainfall and topography reveals a clear spatial relationship between elevation variability and precipitation distribution along the Bukit Barisan mountain transect (**Fig. 7**). The topographic profile shows a pronounced increase in elevation over the central segment, while the rainfall curve exhibits intensity variations that follow changes in surface relief. Precipitation remains relatively low in the initial segment, then gradually increases as it approaches areas characterized by more complex terrain. Rainfall reaches a primary peak at approximately km 170, with an intensity close to 44 mm.day^{-1}, coinciding with the main slope–ridge segment. Beyond this point, precipitation decreases sharply and reaches a local minimum within the range of km 220–260. Toward the final segment of the transect, rainfall increases again, approaching approximately 41 mm.day^{-1} near km 400. This pattern indicates that rainfall distribution along the cross-section is not uniform but instead forms localized maxima associated with variations in surface morphology, particularly across slope–ridge transition zones.

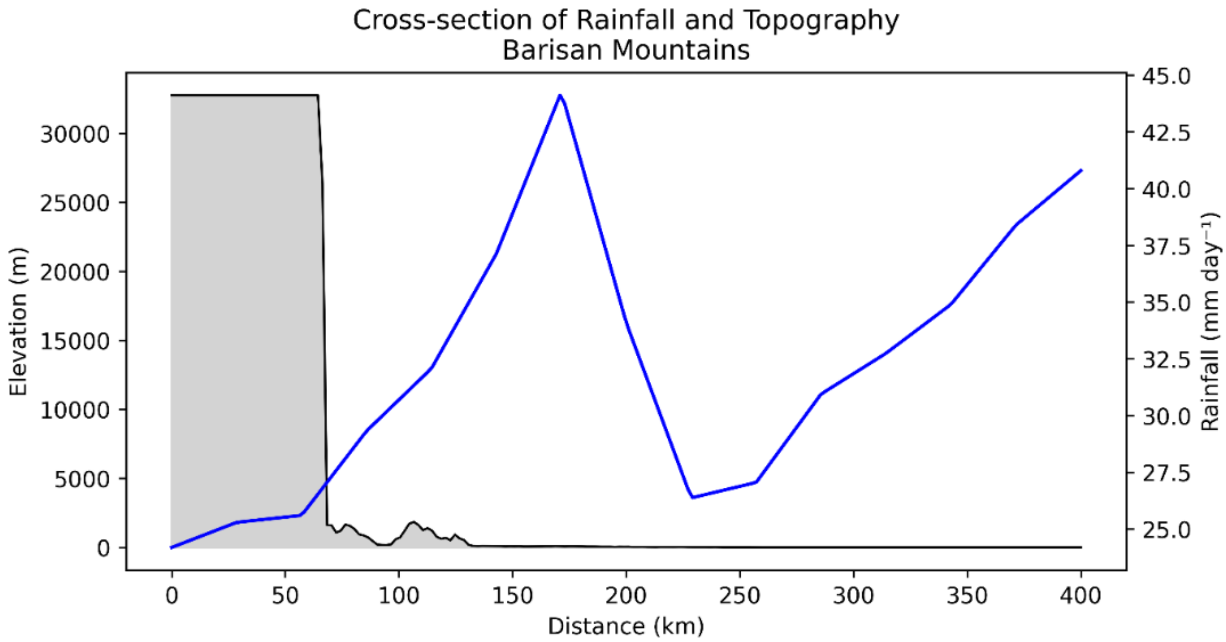

Figure 7. Cross-section of Rainfall and Topography Barisan Mountains

Discussion

The minimum MSLP value of 1009.64 hPa recorded during Tropical Cyclone Senyar indicates the presence of a low-pressure system that effectively organized surface circulation over North Sumatra (Syahreza et al., 2026). The predominance of westerly wind patterns directed toward the western coast reflects the advection of moist air driven by the outer circulation of the cyclone, consistent with the moisture pump mechanism documented in the context of equatorial tropical cyclones (Pérez-Alarcón et al., 2024), (Pérez-Alarcón et al., 2023). The interaction of this moist inflow with the Bukit Barisan Mountain Range amplified the likelihood of orographic lifting and local convergence, thereby promoting significant rainfall enhancement over the Sibolga, North Tapanuli, and Mandailing Natal regions (Houze, 2012), (Wang et al., 2020). Meanwhile, airflow channeled through the Strait of Malacca indicates that moisture supply also extended to the eastern coast, contributing to elevated precipitation over Langkat, Deli Serdang, and Medan (Li et al., 2024). Consequently, the rainfall distribution observed during this event reflects the interaction between regional cyclonic circulation and local topographic controls (Cheng et al., 2025).

The accumulated rainfall distribution over the period of 21-30 November 2026 demonstrates that Tropical Cyclone Senyar produced intense and spatially concentrated precipitation across several sectors of North Sumatra, with total accumulations ranging from 117.16-871.48 mm. Accumulation values exceeding 300 mm across most of the study domain, particularly along the western and eastern coastal sectors, indicate that the system not only triggered intense short-duration rainfall but also sustained moisture supply and convective activity persistently over several days (Deo et al., 2021), (Prat & Nelson, 2016). The maximum daily rainfall of 327.01 mm.day^{-1} further confirms the extreme precipitation character of this event (Yang et al., 2021). The occurrence of daily rainfall ≥150 mm.day^{-1} over Sibolga, North Tapanuli, Langkat, Medan, and Deli Serdang demonstrates that the system's impacts manifested simultaneously across two distinct coastal sectors, reflecting the broad yet dynamically focused influence of the cyclonic system on areas most responsive to moisture supply and atmospheric lifting (Jia et al., 2024).

The fact that both the total rainfall accumulation and the maximum daily rainfall peaked at the same coordinate of 4.50°N, 99.00°E indicates the presence of a precipitation core zone experiencing the most intense rainfall concentration. This suggests that the location was optimally positioned to receive the combined effects of water vapor advection, moisture convergence, and vertical lifting support, rendering it the primary center of rainfall accumulation throughout the duration of the cyclonic influence (Wu et al., 2026). The co-occurrence of strong IVT, organized moisture flux, and localized moisture convergence indicates that rainfall development over North Sumatra was supported by an efficient and sustained regional moisture supply mechanism (Gimeno-Sotelo & Gimeno, 2023), (Raghuvanshi & Agarwal, 2023). The IVT structure suggests that Tropical Cyclone Senyar facilitated the formation of a coherent moisture transport corridor from surrounding ocean bodies toward the study area (Liu et al., 2023), (Yong et al., 2026). Once advected inland, this moisture was concentrated through low-level convergence, providing favorable conditions for vertical uplift and deep convective development (Pérez-Alarcón et al., 2023), (Liu et al., 2023). Therefore, the rainfall event was dynamically sustained not only by local atmospheric instability, but also by large-scale moisture advection and horizontal moisture accumulation a mechanism analogous to that documented in other extreme rainfall cases involving tropical cyclone-associated moisture corridors (Jia et al., 2024), (Cuckow et al., 2024).

The spatial rainfall distribution indicates that topography played a critical role in controlling the location and intensity of precipitation over North Sumatra during the influence of Tropical Cyclone Senyar. The concentration of rainfall in areas characterized by complex relief indicates that precipitation formation was not solely determined by moisture availability, but also by the mechanism of forced ascent resulting from the interaction of moist airflow with surface morphology (Houze, 2012), (Cheng et al., 2025). As the moist air mass driven by cyclonic circulation moved onshore over North Sumatra, it underwent orographic lifting upon encountering the slopes of the Bukit Barisan Range, enhancing adiabatic cooling, accelerating condensation, and promoting the development of deep and persistent convective cloud systems (Wang et al., 2020), (Wu et al., 2026). The elongated rainfall distribution following the topographic orientation indicates that orographic influence is spatially structured. This implies that the mountain range does not function merely as a passive barrier but also acts as a local amplifier of convergence and atmospheric lifting processes (Cuckow et al., 2024). The presence of Tropical Cyclone Senyar directly enhanced moisture supply and strengthened the background flow, rendering topographic effects more efficient in initiating and sustaining precipitation [60], [58].

Differences in rainfall intensity between the mountainous sector and open terrain demonstrate that the atmospheric response to the cyclonic disturbance was spatially heterogeneous across the study domain. Areas topographically favorable for vertical lifting tended to serve as zones of maximum rainfall accumulation, whereas regions outside the primary lifting corridor exhibited considerably weaker precipitation (Li et al., 2024). This pattern is consistent with the rainfall characteristics of maritime tropical environments, where the combination of synoptic-scale forcing and local topographic modification frequently governs the fine-scale distribution of precipitation (Prat & Nelson, 2016), (Yang et al., 2021). From a dynamic meteorological perspective, the rainfall event over North Sumatra during the study period represents the product of multiscale interactions between the regional-scale circulation induced by Tropical Cyclone Senyar and mesoscale-to-local amplification by orography (Narenpitak et al., 2020), (Gorja et al., 2025). The resulting precipitation distribution not only reflects the atmospheric response to a large-scale disturbance but also demonstrates how regional topography governs the efficiency of moisture-to-precipitation conversion (Liu et al., 2023).

The topographic–precipitation cross-section further confirms that orography directly modulated rainfall intensity. Elevated precipitation along segments associated with slopes and ridges indicates orographic lifting as moist airflow was forced upward along the relief of the Barisan Range a mechanism that enhances adiabatic cooling and accelerates condensation (Cheng et al., 2025), [68]. he rainfall peak around km 170 identifies this zone as the area of most effective vertical lifting response along the transect, consistent with globally documented seeder-feeder and orographic flow enhancement mechanisms [54], [68]. The decline in rainfall following the primary peak reflects diminishing lifting efficiency on the lee side of the dominant slope, while the subsequent secondary increase indicates secondary lifting, local convergence, or lee-side moisture redistribution (Wu et al., 2026). Collectively, these findings confirm that the Barisan Range acted as a dynamic amplifier of vertical motion, determining the location of the most intense precipitation accumulation, and that the observed extreme rainfall represents the product of a synergistic interaction between cyclonic synoptic-scale forcing and local orographic mechanisms (Syahreza et al., 2026), (Narenpitak et al., 2020), (Liu et al., 2023).

CONCLUSION

Tropical Cyclone Senyar generated an extreme precipitation event over North Sumatra through a synergistic multiscale interaction between regional cyclonic circulation and local orographic enhancement. The low-pressure system, with a minimum MSLP of 1009.64 hPa, effectively facilitated the formation of a coherent moisture transport corridor from the surrounding ocean bodies toward the landmass, characterized by strong IVT, organized moisture flux, and localized moisture convergence, resulting in total rainfall accumulations of 117.16-871.48 mm and a maximum daily rainfall of 327.01 mm.day^{-1} over the period of 21-30 November 2026. The resulting precipitation distribution, concentrated within a core zone at 4.50°N, 99.00°E and extending asymmetrically toward both the western and eastern coastal sectors, was not a uniform response to the large-scale disturbance. Rather, it reflects how the Bukit Barisan Mountain Range actively amplified vertical dynamics through forced ascent, adiabatic cooling, and local convergence, such that areas situated along the optimal lifting corridor experienced substantially more intense precipitation accumulation than surrounding regions. This event therefore unequivocally demonstrates that the distribution of extreme rainfall in maritime tropical environments is governed not by any single factor in isolation, but by the integrated coupling of synoptic-scale cyclonic forcing which persistently supplies moisture and mesoscale-to-local topographic modulation which converts that moisture into precipitation with high efficiency.

ACKNOWLEDGMENT

The author would like to express sincere gratitude to Meteorology, Climatology, and Geophysical Agency for providing the actual event data used in this study.

AUTHOR CONTRIBUTION STATEMENT

MA conducted all aspects of the research, including data processing, analysis, and manuscript writing.

CONFLICTS OF INTEREST

The author declares no conflict of interest.

INFORMED CONSENT STATEMENT

Not applicable.

USE OF ARTIFICIAL INTELLIGENCE (AI)-ASSISTED TECHNOLOGY

During the preparation of this work, the author used Claude AI to assist in developing data processing scripts. After using this tool, the author reviewed and edited the content as needed and takes full responsibility for the content of the publication.

REFERENCES

Abdillah, M. R., Jannatunnisa, L., Purwadani, N. N., Nugraha, D., Fajary, F. R., Putri, N. S., Prawira, R. D., Junnaedhi, I. D. G. A., Riawan, E., & Aminah, S. (2026). Synoptic Drivers of Tropical Cyclone Senyar and Long-term Change in Near-Equatorial Tropical Cyclones over the Maritime Continent.. https://doi.org/10.22541/essoar.177248986.68667068/v1

Arakane, S., Hsu, H. H., Tu, C. Y., Liang, H. C., Yan, Z. Y., & Lin, S. J. (2019). Remote effect of a tropical cyclone in the Bay of Bengal on a heavy-rainfall event in subtropical East Asia. npj Climate and Atmospheric Science, 2(1), 25. https://doi.org/10.1038/s41612-019-0082-8

Balaji, M., Chakraborty, A., & Mandal, M. (2018). Changes in tropical cyclone activity in north Indian Ocean during satellite era (1981–2014). International Journal of Climatology, 38(6), 2819–2837. https://www.researchgate.net/profile/Balaji-Mani-

2/publication/323580959_Changes_in_tropical_cyclone_activity_in_north_Indian_Ocean_during_satellite_era_1981-2014/links/5aa4305aa6fdccd544baa32c/Changes-in-tropical-cyclone-activity-in-north-Indian-Ocean-during-satellite-era-1981-2014.pdf

Bracewell, R. N., & Bracewell, R. N. (1986). The Fourier transform and its applications. McGraw-hill New York. https://aeb.gov.lk/wp-content/uploads/2023/04/ryo-lf-pvgly-the-fourier-transform-and-its-applications-13247253-nrotb.pdf

Chakraborty, S., Pattnaik, S., & Kannan, B. A. M. (2026). Influence of inner-core dynamics regulating the intensity decay of landfalling tropical cyclones over the eastern coast of India. Quarterly Journal of the Royal Meteorological Society, e70160. https://doi.org/10.1002/qj.70160

Chen, H. C. (2025). Mechanisms of Topographic Steering and Track Morphology of Typhoon-like Vortices over Complex Terrain: A Dynamic Model Approach. Atmosphere, 17(1), 60. https://doi.org/10.3390/atmos17010060

Chen, J., Tam, C. Y., Cheung, K., Wang, Z., Murakami, H., Lau, N. C., Garner, S. T., Xiao, Z., Choy, C. W., & Wang, P. (2021). Changing Impacts of Tropical Cyclones on East and Southeast Asian Inland Regions in the Past and a Globally Warmed Future Climate. Frontiers in Earth Science, 9. https://doi.org/10.3389/feart.2021.769005

Chen, R., Xu, H., & Xu, X. (2026). Impact of deep-inland typhoon track uncertainty on the 2023 record-breaking rainfall over North China: an ensemble-based analysis. Environmental Research Letters. https://doi.org/10.1088/1748-9326/ae51ab DownloadArticle PDF

Cheng, L. W., Yu, C. K., & Chen, S. P. (2025). Identifying mechanisms of tropical cyclone generated orographic precipitation with Doppler radar and rain gauge observations. npj Climate and Atmospheric Science, 8(1), 35. https://doi.org/10.1038/s41612-025-00921-4

Cornes, R. C., Jones, P. D., Briffa, K. R., & Osborn, T. J. (2012). A daily series of mean sea-level pressure for London, 1692–2007. International Journal of Climatology, 32(5), 641-656. https://doi.org/10.1002/joc.2301

Cuckow, S., Dacre, H. F., Martínez-Alvarado, O., & Smith, S. A. (2024). Quantifying the Role of Orographic Processes in Producing Extreme Precipitation: A Case Study of an Atmospheric River Associated With Storm Bronagh. Journal of Geophysical Research: Atmospheres, 129(18), e2023JD040557. https://doi.org/10.1029/2023JD040557

Day, J., Chin, N., Sydnor, S., & Cherkauer, K. (2013). Weather, climate, and tourism performance: A quantitative analysis. Tourism Management Perspectives, 5, 51–56. https://www.sciencedirect.com/science/article/pii/S221197361200089X

Deo, A., Chand, S. S., Ramsay, H., Holbrook, N. J., McGree, S., Magee, A., Bell, S., Titimaea, M., Haruhiru, A., Malsale, P., Mulitalo, S., Daphne, A., Prakash, B., Vainikolo, V., & Koshiba, S. (2021). Tropical cyclone contribution to extreme rainfall over southwest Pacific Island nations. Climate Dynamics, 56(11), 3967-3993. https://doi.org/10.1007/s00382-021-05680-5

Deshpande, M., Singh, V. K., Ganadhi, M. K., Roxy, M. K., Emmanuel, R., & Kumar, U. (2021). Changing status of tropical cyclones over the north Indian Ocean. Climate Dynamics, 57(11-12), 3545-3567. https://doi.org/10.1007/s00382-021-05880-z

French, J. R., Friedrich, K., Tessendorf, S. A., Rauber, R. M., Geerts, B., Rasmussen, R. M., Xue, L., Kunkel, M. L., & Blestrud, D. R. (2018). Precipitation formation from orographic cloud seeding. Proceedings of the National Academy of Sciences, 115(6), 1168-1173. https://doi.org/10.1073/pnas.1716995115

Gimeno-Sotelo, L., & Gimeno, L. (2023). Where does the link between atmospheric moisture transport and extreme precipitation matter?. Weather and Climate Extremes, 39, 100536. https://doi.org/10.1016/j.wace.2022.100536

Glaskova, T. I., Guedes, R. M., Morais, J. J., & Aniskevich, A. N. (2007). A comparative analysis of moisture transport models as applied to an epoxy binder. Mechanics of Composite Materials, 43(4), 377-388. https://doi.org/10.1007/s11029-007-0034-y

Gorja, M. M. K., Vissa, N. K., & Viswanadhapalli, Y. (2025). Multi-scale atmospheric interactions and their role in modulating pre-monsoon tropical cyclone movement: a regional modeling approach. Climate Dynamics, 63(9), 366. https://doi.org/10.1007/s00382-025-07800-x

Hoarau, K., Bernard, J., & Chalonge, L. (2012). Intense tropical cyclone activities in the northern Indian Ocean. International journal of climatology, 32(13), 1935–1945. https://www.researchgate.net/profile/Karl-Hoarau/publication/257829260_Intense_tropical_cyclone_activities_in_the_northern_Indian_Ocean

/links/59fb569eaca272347a1d69b3/Intense-tropical-cyclone-activities-in-the-northern-Indian-Ocean.pdf
Houze, R. A. (2012). Orographic effects on precipitating clouds. Reviews of Geophysics, 50(1), 2011RG000365. https://doi.org/10.1029/2011RG000365
Jia, L., Ren, F., McBride, J. L., & Cong, C. (2024). Characteristics and Preliminary Causes of Tropical Cyclone Remote Precipitation over China. Journal of Ocean University of China, 23(4), 845-858. https://doi.org/10.1007/s11802-024-5760-4
Junquas, C., Takahashi, K., Condom, T., Espinoza, J. C., Chavez, S., Sicart, J. E., & Lebel, T. (2018). Understanding the influence of orography on the precipitation diurnal cycle and the associated atmospheric processes in the central Andes. Climate Dynamics, 50(11-12), 3995-4017. https://doi.org/10.1007/s00382-017-3858-8
Katru, N., Joseph, S., Sripathi, G., Raju, A. D., Mohapatra, M., Suneetha, P., Kumar, S. V. J., Kant, S., & SH, B. (2025). Key factors behind super cyclone Gonu (1–7 June 2007) over the Arabian Sea. Mausam, 76(4), 1035–1046. https://doi.org/10.54302/mausam.v76i4.7095
Khouakhi, A., Villarini, G., & Vecchi, G. A. (2017). Contribution of Tropical Cyclones to Rainfall at the Global Scale.. https://doi.org/10.1175/JCLI-D-16-0298.1
Kidder, S. Q., Goldberg, M. D., Zehr, R. M., DeMaria, M., Purdom, J. F. W., Velden, C. S., Grody, N. C., & Kusselson, S. J. (2000). Satellite Analysis of Tropical Cyclones Using the Advanced Microwave Sounding Unit (AMSU). Bulletin of the American Meteorological Society, 81(6), 1241-1259. https://doi.org/10.1175/1520-0477(2000)081<1241:SAOTCU>2.3.CO;2
Kim, E. T., Kim, J. H., Kim, S. M., & Lim, Y. J. (2025). Orographic and Coastal Impacts on the Unexpected Development of the Snowstorm in Seoul Metropolitan Area. Available at SSRN 5929746. https://papers.ssrn.com/sol3/papers.cfm?abstract_id=5929746
Klotzbach, P. J., Wood, K. M., Schreck III, C. J., Bowen, S. G., Patricola, C. M., & Bell, M. M. (2022). Trends in Global Tropical Cyclone Activity: 1990–2021. Geophysical Research Letters, 49(6), e2021GL095774. https://doi.org/10.1029/2021GL095774
Lentink, H. S., Grams, C. M., Riemer, M., & Jones, S. C. (2018). The Effects of Orography on the Extratropical Transition of Tropical Cyclones: A Case Study of Typhoon Sinlaku (2008).. https://doi.org/10.1175/MWR-D-18-0150.1
Leroux, M. D., Wood, K., Elsberry, R. L., Cayanan, E. O., Hendricks, E., Kucas, M., Otto, P., Rogers, R., Sampson, B., & Yu, Z. (2018). Recent advances in research and forecasting of tropical cyclone track, intensity, and structure at landfall. Tropical Cyclone Research and Review, 7(2), 85–105. https://doi.org/10.6057/2018TCRR02.02
Li, X., Lu, R., Chen, G., & Chen, R. (2024). Western North Pacific tropical cyclones suppress Maritime Continent rainfall. npj Climate and Atmospheric Science, 7(1), 251. https://doi.org/10.1038/s41612-024-00810-2
Liu, T., Chen, Y., Chen, S., Li, W., & Zhang, A. (2023). Mechanisms of the transport height of water vapor by tropical cyclones on heavy rainfall. Weather and Climate Extremes, 41, 100587. https://doi.org/10.1016/j.wace.2023.100587
Lui, Y. S., Chong, M. L., Ho, C. K., Tang, W. H., Yeung, H. Y., Tse, W. P., Lai, K. K., & Chan, P. W. (2026). Tropical Storm Senyar—The First Observed Tropical Cyclone Forming over the Strait of Malacca and Moving Eastwards into the South China Sea. Atmosphere, 17(3), 275. https://doi.org/10.3390/atmos17030275
Mazza, E., & Chen, S. S. (2023). Tropical Cyclone Rainfall Climatology, Extremes, and Flooding Potential from Remote Sensing and Reanalysis Datasets over the Continental United States.. https://doi.org/10.1175/JHM-D-22-0199.1
Narenpitak, P., Bretherton, C. S., & Khairoutdinov, M. F. (2020). The Role of Multiscale Interaction in Tropical Cyclogenesis and Its Predictability in Near-Global Aquaplanet Cloud-Resolving Simulations.. https://doi.org/10.1175/JAS-D-20-0021.1
Needham, H. F., Keim, B. D., & Sathiaraj, D. (2015). A review of tropical cyclone-generated storm surges: Global data sources, observations, and impacts. Reviews of Geophysics, 53(2), 545-591. https://doi.org/10.1002/2014RG000477
Pérez-Alarcón, A., Coll-Hidalgo, P., Fernández-Alvarez, J. C., Trigo, R. M., Nieto, R., & Gimeno, L. (2023). Impacts of tropical cyclones on the global water budget. npj Climate and Atmospheric Science, 6(1), 212. https://doi.org/10.1038/s41612-023-00546-5

Pérez-Alarcón, A., Fernández-Alvarez, J. C., Trigo, R. M., Nieto, R., & Gimeno, L. (2024). Insights into the origin of precipitation moisture for tropical cyclones during rapid intensification process. Tropical Cyclone Research and Review, 13(2), 72-87. https://doi.org/10.1016/j.tcrr.2024.05.001
Prat, O. P., & Nelson, B. R. (2016). On the Link between Tropical Cyclones and Daily Rainfall Extremes Derived from Global Satellite Observations.. https://doi.org/10.1175/JCLI-D-16-0289.1
Purkis, S. J., & Klemas, V. V. (2011). Remote sensing and global environmental change. John Wiley & Sons. https://books.google.com/books?hl=id&lr=&id=VKoGbuTEODoC&oi=fnd&pg=PA1&dq=Remote+Sensing+of+the+Environment&ots=4YmeHOSRfG&sig=ycwfD9_r4BfumOK45M5kexxhndw
Raghuvanshi, S. A., & Agarwal, A. (2023). Unraveling atmospheric moisture transport linkages to extreme precipitation events and associated synoptic features over India. Journal of Hydrology, 626, 130290. https://doi.org/10.1016/j.jhydrol.2023.130290
Rahman, S., Sharmin, N., Rahat, A., Rahman, M., & Rahman, M. (2024). Tropical cyclone warning and forecasting system in Bangladesh: challenges, prospects, and future direction to adopt artificial intelligence. Computational Urban Science, 4(1), 4. https://doi.org/10.1007/s43762-023-00113-x
Ramadhan, N., Dwipa, I., Muhsanati, M., Sari, W. P., Sari, A., Amanda, S., Nugroho, D., Ramadhan, R. D., & Saputra, R. A. (2026). CHIRPS-Based Spatio-Temporal Rainfall Analysis as a Basis for Evaluating Cropping Pattern Suitability in Coastal West Sumatra. Journal of Applied Agricultural Science and Technology, 10(1), 146–158. https://doi.org/10.55043/jaast.v10i1.524
Sandu, I., Niekerk, A., Shepherd, T. G., Vosper, S. B., Zadra, A., Bacmeister, J., Beljaars, A., Brown, A. R., Dörnbrack, A., & McFarlane, N. (2019). Impacts of orography on large-scale atmospheric circulation. npj Climate and Atmospheric Science, 2(1), 10. https://doi.org/10.1038/s41612-019-0065-9
Schumacher, R. S., & Rasmussen, K. L. (2020). The formation, character and changing nature of mesoscale convective systems. Nature Reviews Earth & Environment, 1(6), 300–314. https://doi.org/10.1038/s43017-020-0057-7
Sheil, D. (2026). How Forests May Reduce the Incidence of Destructive Tropical Cyclones, Hurricanes and Typhoons. Forests, 17(3), 359. https://doi.org/10.3390/f17030359
Shu, S., Feng, X., & Wang, Y. (2018). Essential Role of Synoptic Environment on Rainfall Distribution of Landfalling Tropical Cyclones Over China. Journal of Geophysical Research: Atmospheres, 123(20). https://doi.org/10.1029/2018JD028842
Singh, O. P., Ali Khan, T. M., & Rahman, M. S. (2000). Changes in the frequency of tropical cyclones over the North Indian Ocean. Meteorology and Atmospheric Physics, 75(1-2), 11-20. https://doi.org/10.1007/s007030070011
Smith, P. J. (1971). An analysis of kinematic vertical motions. Monthly Weather Review, 99(10), 715–724. https://journals.ametsoc.org/view/journals/mwre/99/10/1520-0493_1971_099_0715_aaokvm_2_3_co_2.xml
Sobel, A. H., Wing, A. A., Camargo, S. J., Patricola-DiRosario, C. M., Vecchi, G. A., Lee, C., & Tippett, M. K. (2021). Tropical Cyclone Frequency. Earth's Future, 9(12), e2021EF002275. https://doi.org/10.1029/2021EF002275
Suhardi, B., Adiputra, A., & Reeva Avrian (2020). Kajian Dampak Cuaca Ekstrem Saat Siklon Tropis Cempaka dan Dahlia di Wilayah Jawa Barat. Jurnal Geografi, Edukasi dan Lingkungan (JGEL), 4(2), 61-67. https://doi.org/10.29405/jgel.v4i2.4354
Surinati, D., & Kusuma, D. A. (2018). Karakteristik dan Dampak Siklon Tropis yang Tumbuh di Sekitar Wilayah Indonesia. Oseana, 43(2), 1–12. https://www.academia.edu/download/69827498/16.pdf
Syahreza, S., Syukri, M., Qalbi, H. B., Farhan, A., & Cahyo, E. (2026). Brief communication: Extreme rainfall–driven flooding associated with the equatorial development of Tropical Cyclone Senyar in Aceh, Indonesia. EGUsphere, 2026, 1–15. https://egusphere.copernicus.org/preprints/2026/egusphere-2026-694/
Vo, T. H., & Liou, Y. A. (2024). Tropical cyclone-induced rainfall variability and its implications for drought in Taiwan: insights from 1981 to 2022. Atmospheric Research, 312, 107771. https://doi.org/10.1016/j.atmosres.2024.107771
Wadler, J. B., Rudzin, J. E., Jaimes de la Cruz, B., Chen, J., Fischer, M., Chen, G., Qin, N., Tang, B., & Li, Q. (2023). A review of recent research progress on the effect of external influences on tropical cyclone intensity change. Tropical Cyclone Research and Review, 12(3), 200-215. https://doi.org/10.1016/j.tcrr.2023.09.001

Wang, C. C., Ma, S. K., & Johnson, R. H. (2020). A Numerical Study on the Influences of Sumatra Topography and Synoptic Features on Tropical Cyclone Formation over the Indian Ocean.. https://doi.org/10.1175/MWR-D-19-0259.1

Wang, Y., & Wu, C. C. (2004). Current understanding of tropical cyclone structure and intensity changes ? a review. Meteorology and Atmospheric Physics, 87(4), 257-278. https://doi.org/10.1007/s00703-003-0055-6

Wilks, D. S. (2011). Statistical methods in the atmospheric sciences. Academic press. https://books.google.com/books?hl=id&lr=&id=fxPiH9Ef9VoC&oi=fnd&pg=PP1&dq=Statistical+Methods+in+the+Atmospheric+Sciences&ots=ILqhRxk0Ty&sig=kzvJ6jbYr17t6gPFp3rE6srnOCU

Wu, H., Gao, H., Huang, Y., & Xu, C. (2026). Analysis of the Compound Disaster Caused by Extreme Rainfall and Landslides in Sumatra, Indonesia in 2025 and Its Implications for Disaster Prevention and Mitigation. Natural Hazards Research. https://doi.org/10.1016/j.nhres.2026.03.003

Yang, B. (2026). The Control of Tropical Cyclone Wind Structure on Inner and Outer Rainband Formation: A Balanced Dynamics Perspective. Journal of the Atmospheric Sciences, e250185. https://doi.org/10.1175/JAS-D-25-0185.1

Yang, S., Lao, V., Bankert, R., Whitcomb, T. R., & Cossuth, J. (2021). Improved Climatology of Tropical Cyclone Precipitation from Satellite Passive Microwave Measurements. Journal of Climate, 34(11), 4521-4537. https://doi.org/10.1175/JCLI-D-20-0196.1

Yong, Y., Yang, K., & Liang, J. (2026). The role of atmospheric river in the unprecedented extreme precipitation event over Henan in July 2021. Atmospheric Research, 336, 108877. https://doi.org/10.1016/j.atmosres.2026.108877

Zhi-ying, D., Xiao-hui, Z., Rui, X., & Yong, G. A. O. (2017). Statistical analysis of summer tropical cyclone remote precipitation events in East Asia from 2000 to 2009 and numerical simulation. Journal of Tropical Meteorology, 23(1), 37–46. https://jtm.itmm.org.cn/article/doi/10.16555/j.1006-8775.2017.01.004

Zhou, T., Zhang, L., & Li, H. (2008). Changes in global land monsoon area and total rainfall accumulation over the last half century. Geophysical Research Letters, 35(16). https://doi.org/10.1029/2008GL034881